Articles

Templated Synthesis of Pyridine Functionalized Mesoporous Carbons through the Cyclotrimerization of Diethynylpyridines†

Yongsoon Shin and Glen E. Fryxell*

Pacific Northwest National Laboratory, P. O. Box 999, Richland, Washington 99352

Charles A. Johnson II and Michael M. Haley

Department of Chemistry and the Materials Science Institute, University of Oregon, Eugene, Oregon 97403-1253

Received April 9, 2007. Revised Manuscript Received June 8, 2007

Templated mesoporous carbons designed around the pyridine functionality have been made using the cyclotrimerization of a variety of diethynylpyridines. The substitution pattern of the ethynyl moieties about the pyridine ring system was found to have a significant impact on the structure and properties of the final product. A model is proposed that focuses on the self-assembly of the diethynylpyridine monomer on the silica surface and the order and orientation of the ethynyl moieties within this monolayer.

Introduction

The templated synthesis of mesoporous carbon has been an active area of research now for several years.[1–19] Generally this chemistry has involved deposition of a precursor species into the pores of a suitable template (e.g., mesoporous silica) to create an organized pre-assembly complex, followed by some sort of polymerization chemistry, and finishing up with a carbonization step. The polymerization chemistry used has included charring of sugars,[1] electrophilic aromatic substitution (e.g., Friedel−Crafts alkylation),[2] and polymerization of phenol[3] or other aromatic hydrocarbons,[4] as well as using phenolic resin,[5] pitch,[6] and colloidal carbon[7] as the carbon precursor. In addition, heterocyclic precursors have been used in this chemistry (e.g., furan derivatives[8]), and nitrogen-based functionality has been introduced using poly(arylonitrile),[9] and poly(pyrrole)[10] to make these mesoporous carbons. N-doped mesoporous carbons have been made using other strategies as well.[11,12] A potential weakness of using a carbon precursor derived from olefin polymerization or Friedel−Crafts alkylation (or acylation) chemistry is that these reactions are known to be reversible, leading to the potential of depolymerization during the carburization step. This can lead to structural defects or loss of functionality. The charring or pitch approaches severely limit the functionality that can be incorporated into the final mesoporous carbon product.

The value of surface functionalized mesoporous carbon (FMC) has been recognized, and efforts have been made to prepare these materials.[13] N-doped mesoporous carbons with 6.5–8 wt% N have been made using chemical vapor deposition of acetonitrile into a mesoporous silica template at 900–1000 °C.[11,12] These N-doped materials were found to be composed of hollow spheres and to have surface areas as high as 1019 m^2/g and pore volumes of as much as 0.83 cm^3/g. X-ray photoelectron spectroscopy (XPS) analysis of the N content suggested a mixture of quaternary ammonium salts and "pyridine-like" (i.e., sp^2 hybridized) N atoms.[11,12] We have devised an alternate synthetic strategy to make

† Part of the "Templated Materials Special Issue".

* Corresponding author: tel.: 509-375-3856; e-mail: glen.fryxell@pnl.gov.

(1) Ryoo, R.; Joo, S. H.; Jun, S. *J. Phys. Chem. B* **1999**, *103*, 7743–7746.
(2) Joo, S. H.; Choi, S. J.; Oh, I.; Kwak, J.; Liu, Z.; Terasaki, O.; Ryoo, R. *Nature* **2001**, *412*, 169–172.
(3) Lee, J.; Sohn, K.; Hyeon, T. *J. Am. Chem. Soc.* **2001**, *123*, 5146–5147.
(4) Kim, C. H.; Lee, D.-K.; Pinnavaia, T. J. *Langmuir* **2004**, *20*, 5157–5159.
(5) Gierszal, K. P.; Jaroniec, M. *J. Am. Chem. Soc.* **2006**, *128*, 10026–10027.
(6) Li, Z.; Jaroniec, M. *J. Phys. Chem. B* **2004**, *108*, 824–826.
(7) Li, Z.; Jaroniec, M. *J. Am. Chem. Soc.* **2001**, *123*, 9208–9209.
(8) Kawashima, D.; Aihara, T.; Kobayashi, Y.; Kyotani, T.; Tomita, A. *Chem. Mater.* **2000**, *12*, 3397–3401.
(9) Lu, A. H.; Kiefer, A.; Schmidt, W.; Schüth, F. *Chem. Mater.* **2004**, *16*, 100–103.
(10) Yang, C.-M.; Weidenthaler, C.; Spliethoff, B.; Mayanna, M.; Schuth, F. *Chem. Mater.* **2005**, *17*, 355–358.
(11) Xia, Y.; Yang, Z.; Mokaya, R. *J. Phys. Chem. B* **2004**, *108*, 19293–19298.
(12) Xia, Y.; Mokaya, R. *Chem. Mater.* **2005**, *17*, 1553–1560.
(13) Li, Z.; Yan, W.; Dai, S. *Langmuir* **2005**, *21*, 11999–12006.
(14) Liang, C.; Dai, S. *J. Am. Chem. Soc.* **2006**, *128*, 5316–5317.
(15) Sayari, A.; Yang, Y. *Chem. Mater.* **2005**, *17*, 6108–6113.
(16) Huang, L.; Wind, S. J.; O'Brien, S. P. *Nano Lett.* **2003**, *3*, 299–303.
(17) Kruk, M.; Jaroniec, M.; Ryoo, R.; Joo, S. H. *J. Phys. Chem. B* **2000**, *104*, 7960–7968.
(18) Meng, Y.; Gu, D.; Zhang, F.; Shi, Y.; Cheng, L.; Feng, D.; Wu, Z.; Chen, Z.; Wan, Y.; Stein, A.; Zhao, D. *Chem. Mater.* **2006**, *18*, 4447–4464.
(19) Shin, Y.; Fryxell, G. E.; Um, W.; Parker, K.; Mattigod, S. V.; Skaggs, R. Sulfur Functionalized Mesoporous Carbon. *Adv. Funct. Mater.*,in press.

10.1021/cm070979o CCC: $40.75
Published on Web 08/23/2007

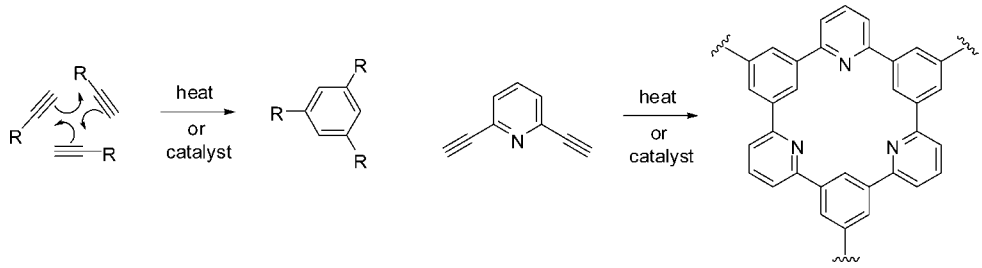

Figure 1. Cyclotrimerization of acetylenes to form substituted benzenes and how the cyclotrimerization of diethynylpyridines might be used to form functionalized mesoporous carbons built around the pyridine ring system (Pyr-FMCs).

inherently functional mesoporous carbons by using heteroaromatic precursors to create a backbone built around specific heteroaromatic functionality.[19] For example, these sulfur-functionalized mesoporous carbons (S-FMCs) have been made using a linear polymerization of (2-thiophenemethanol) using Friedel−Crafts alkylation chemistry.[19]

It would be advantageous if such a strategy could be coupled with dendritic polymerization (as opposed to linear polymerization), to increase the degree of crosslinking and thereby the stability of the backbone structure. Cyclotrimerization of acetylenes forms trisubstituted benzene rings (see Figure 1) and is therefore not easily reversible or prone to depolymerization.[20–31] This is important as the carbonization conditions can lead to a loss of functionality for those systems in which the depolymerization or fragmentation is readily available. Cyclotrimerization should inherently produce a high degree of crosslinking, resulting in a carbon backbone that is thermally quite robust. The cyclotrimerization chemistry is typically performed with a transition metal catalyst (commonly Ni, Co, Rh, or Ir)[20–29] but can also be performed thermally.[30,31] For unsymmetrical acetylenes, a mixture of isomers is possible, but generally speaking the 1,2,4- or 1,3,5-isomers are observed (depending on the steric nature of the acetylene substituents). Cyclotrimerization has been used to make a variety of highly congested arenes (e.g. hexaisopropylbenzene),[23] making it well-suited for this sort of dendritic polymerization chemistry. In this manuscript, we report the synthesis of inherently functional mesoporous carbons using the cyclotrimerization of heteroarylacetylenes to create carbon frameworks that are built around specific heteroaromatic functionality (a pyridine ring).

Experimental Section

Solvents and reagents were purchased commercially (Aldrich) and, unless noted otherwise, were used without further purification. Organic precursors were characterized by ^{1}H NMR, and spectral details were consistent with previously reported values. Mesoporous carbons were characterized by BET surface area analysis, X-ray diffraction (XRD), XPS, and transmission electron microscopy (TEM). Before the BET analysis (carried out on a Quantachrome Autosorb-6), each sample was degassed at 100 °C overnight under vacuum of about 10^{-3} Torr. BET surface areas, pore volumes, and pore size distributions were determined from N_2 adsorption isotherms. Adsorption data in the range of relative pressures $P/P_0 = 0.05–0.15$ were used to calculate the BET surface area. Pore size distributions were calculated from adsorption branches of the N_2 isotherm using the BJH method. XRD patterns of the samples were obtained on a Philips X'ert MPD X-ray diffractomer using Cu Kα (1.54059 Å) radiation with the X-ray generator operating at 45 kV and 40 mA. XPS measurements were performed using a Physical Electronics Quantum 2000 Scanning ESCA Microprobe. This system uses a focused monochromatic Al Kα X-ray (1486.7 eV) source and a spherical section analyzer. TEM images were obtained on a JEOL JEM 2010 microscope. The TEM sample was prepared by dropping a sample suspended in ethanol on a Cu grid coated with carbon films.

General Procedure for Bis(trimethylsilylethynyl)pyridine Formation. A suspension consisting of dibromopyridine (1 equiv), $PdCl_2(PPh_3)_2$ (10 mol%), and CuI (20 mol%) in tetrahydrofuran and *i*-Pr_2NH (1:1 ratio, 0.15 M) was degassed by bubbling argon for 20 min. The reaction mixture was placed under N_2 and heated to 50 °C. Trimethylsilylacetylene (TMSA; 2.5 equiv) was added via syringe, and the reaction mixture was stirred for 6 h. The mixture was concentrated and filtered through a 2.5 cm silica plug with 1:1 hexanes/CH_2Cl_2. Concentration of the filtrate followed by recrystallization with EtOH afforded the bis(TMS-protected)diethynylpyridine (2,5-, 79%; 2,6-, 81%; 3,5-, 75%) as light tan crystals. The spectral data were in accord with those reported in the literature.[32–34]

General Procedure for Diethynylpyridine Formation. A suspension consisting of the bis(TMS-protected)diethynylpyridine (1 equiv) and K_2CO_3 (3–5 equiv) in Et_2O and MeOH (1:2 ratio, 0.05 M) was stirred at ambient temperature for 1 h. The suspension was diluted with Et_2O and washed three times with H_2O and once with brine. The organic layer was dried over $MgSO_4$ and concentrated in vacuo to afford the diethynylpyridine (2,5-, 97%; 2,6-, 99%; 3,5-, 97%) as a light brown solid. The spectral data were in accord with those reported in the literature.[32–34]

(20) Vollhardt, K. P. C. *Angew. Chem., Int. Ed. Engl.* **1984**, *23*, 539–556.
(21) Vollhardt, K. P. C. *Acc. Chem. Res.* **1977**, *10*, 1–8.
(22) For a general discussion of the cyclotrimerization of alkynes, see: March, J. *Advanced Organic Chemistry*, 4th ed.; John Wiley and Sons: New York, 1992; pp 873–875.
(23) Arnett, E. M.; Bollinger, J. M. *J. Am. Chem. Soc.* **1964**, *86*, 4729–4731.
(24) Holmblad, P. M.; Rainer, D. R.; Goodman, D. W. *J. Phys. Chem. B* **1997**, *101*, 8883–8886.
(25) McAlister, D. R.; Bercaw, J. E.; Bergman, R. G. *J. Am. Chem. Soc.* **1977**, *99*, 1666–1668.
(26) Ferrari, A. M.; Giordano, L.; Pacchioni, G.; Abbet, S.; Heiz, U. *J. Phys. Chem. B* **2002**, *106*, 3173–3181.
(27) Patterson, C. H.; Lambert, R. M. *J. Phys. Chem.* **1988**, *92*, 1266–1270.
(28) Lambregts, M. J.; Munson, E. J.; Kheir, A. A.; Haw, J. F. *J. Am. Chem. Soc.* **1992**, *114*, 6875–6879.
(29) Abbet, S.; Sanchez, A.; Heiz, U.; Schneider, W.-D.; Ferrari, A. M.; Pacchioni, G.; Rosch, N. *J. Am. Chem. Soc.* **2000**, *122*, 3453–3457.
(30) Viehe, H. G.; Merenyi, R.; Oth, J. F. M.; Valange, P. *Angew. Chem., Int. Ed. Engl.* **1964**, *3*, 746.
(31) Viehe, H. G.; Merenyi, R.; Oth, J. F. M.; Senders, J. R.; Valange, P. *Angew. Chem., Int. Ed. Engl.* **1964**, *3*, 755–756.
(32) 2,6-Diethynylpyridine: Dana, B. H.; Robinson, B. H.; Simpson, J. *J. Organomet. Chem.* **2002**, *648*, 251–269.
(33) 3,5-Diethynylpyridine: Bosch, E.; Barnes, C. L. *Organometallics* **2000**, *19*, 5522–5524.
(34) (a) 2,5-Diethynylpyridine: Bunten, K. A.; Kakkar, A. K. *Macromolecules* **1996**, *29*, 2885–2893. (b) Gelman, D.; Tsvelikhovsky, D.; Molander, G. A.; Blum, J. *J. Org. Chem.* **2002**, *67*, 6287–6290.

Table 1. Summary of the Properties of the Pyridine-Functionalized Mesoporous Carbons (Pyr-FMCs)

	surface area (m^2/g)	primary pore size (nm)	pore volume (cm^3/g)
Pyr-FMC-1 (2,6)	1180	3.5	0.796
Pyr-FMC-2 (3,5)	1380	3.5	1.47
Pyr-FMC-3 (2,5)	1930	3.0	2.14

Mesoporous Carbon Synthesis. We used SBA-15[15,35] as a template in the synthesis of these mesoporous carbon materials. The SBA-15 used in these syntheses had a surface area of 903 m^2/g, a pore volume of 1.37 cm^3/g, and an average pore size of 9.3 nm (see Supporting Information). The method of incipient wetness was used to introduce the diethynylpyridines into the mesoporous silica template. Thus, 0.70 g of the diethynylpyridine was dissolved in 2.0 mL of acetone and infiltrated into 1.0 g of SBA-15 in 0.5 mL aliquots, with the sample being heated to 80 °C after the addition of each aliquot. This was repeated four times (the sample was noted to turn from white, to brown, to black). The diethynylpyridine laden silica was then heated at 100 °C for 6 h and 800 °C for 2 h. Finally the black silica/carbon composite was washed with 20% HF solution to remove the silica, and the mesoporous carbon product collected by filtration.

Results and Discussion

The intent of this strategy was to prepare regularly ordered structures of pyridine rings linked together through trisubstituted benzene rings (as shown in Figure 1.) While direct thermal cyclotrimerization reactions are relatively rare, we felt that by self-assembling the precursor molecules into an organized array on a silica surface that the entropic issues associated with the cyclotrimerization reaction could be alleviated. The orientation of the pyridine N atom in the final product might also be controlled by varying the substitution pattern of the original diethynylpyridine starting material.

SBA-15[15,35] was chosen as the template for this work and had a surface area of 903 m^2/g, a pore volume of 1.37 cm^3/g, and an average pore size of 9.3 nm (see Supporting Information for adsorption isotherm and pore size distribution). The properties of the pyridine functionalized mesoporous carbons (Pyr-FMCs) obtained via this route are summarized in Table 1. It is immediately apparent from the data in Table 1 that the disposition of the two acetylene units around the pyridine ring system has a significant impact on the structure and properties of the final product. Not surprisingly, all of the products have a notably higher surface area to mass ratio than the starting template (carbon is much lighter than is SiO_2). Also not surprising is the observation that the pore size is smaller than the original template. This is due to the fact that the precursor must sorb to the inside of the template pore walls, leaving the acetylene functionality positioned to result in a much smaller pore diameter than the original pore. It is also important to recognize that the SBA-15 starting material has dense walls, while the product does not, and therefore the spacing between the pores now shows up as a part of the FMC pore structure (and surface area). The wall thickness of a typical SBA-15 sample is about 3.8 nm;[35] measurements on the materials used in these studies revealed a wall thickness of 2.7 nm, and both of these values are similar to the pore sizes observed in these FMCs (3.0–3.5 nm). Pore volume was found to vary considerably from sample to sample and may be due to the formation of multiwalled FMCs, particularly in the case of Pyr-FMC-1 (or possibly due to a partially collapsed mesostructure).

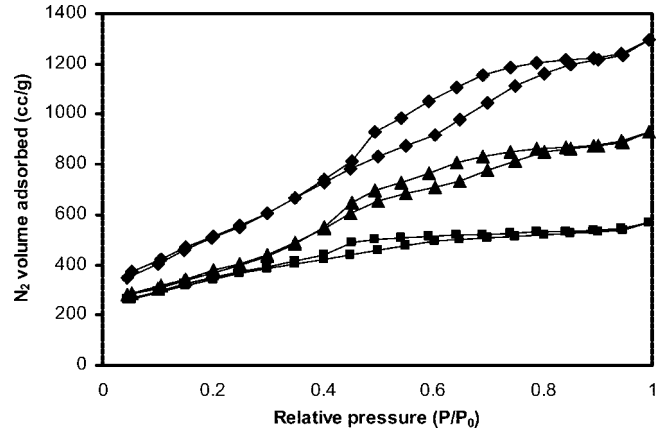

Figure 2. BET adsorption isotherms for the Pyr-FMCs. The squares represent the data for Pyr-FMC-1 (made from 2,6-diethynylpyridine); the triangles represent the data for Pyr-FMC-2 (made from 3,5-diethynylpyridine); and the diamonds represent the data for the Pyr-FMC-3 (made from 2,5-diethynylpyridine).

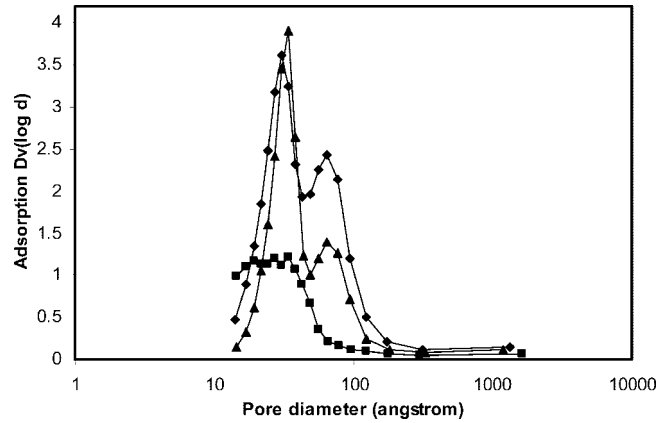

Figure 3. Pore size distributions from the BJH analysis of the adsorption isotherm data for the Pyr-FMCs. The squares represent the data for Pyr-FMC-1 (made from 2,6-diethynylpyridine); the triangles represent the data for Pyr-FMC-2 (made from 3,5-diethynylpyridine); and the diamonds represent the data for the Pyr-FMC-3 (made from 2,5-diethynylpyridine).

The absorption isotherms for the three Pyr-FMCs are shown in Figure 2. The hysteresis observed in these isotherms is indicative of the presence of constrictions within the pores. This is not unexpected as these constrictions are present in the SBA-15 template (see Supporting Information).

The pore size distributions for the three Pyr-FMCs are shown in Figure 3. Consistent with the disordered structure observed in the low angle XRD spectrum (see Figure 4), the pore size distribution for Pyr-FMC-1 is somewhat broad and not as well defined. No larger pores were seen in this sample. The pore size distributions for Pyr-FMC-2 and Pyr-FMC-3 are more sharply defined and have primary pore diameters in the 3.0–3.5 nm range. It is interesting to note that both of these ordered Pyr-FMCs also have a secondary component in their pore structures with a pore diameter of about 7–8 nm. One plausible hypothesis is that this bimodal

(35) Zhao, D.; Huo, Q.; Feng, J.; Chmelka, B. F.; Stucky, G. D. *J. Am. Chem. Soc.* **1998**, *120*, 6024–6036.

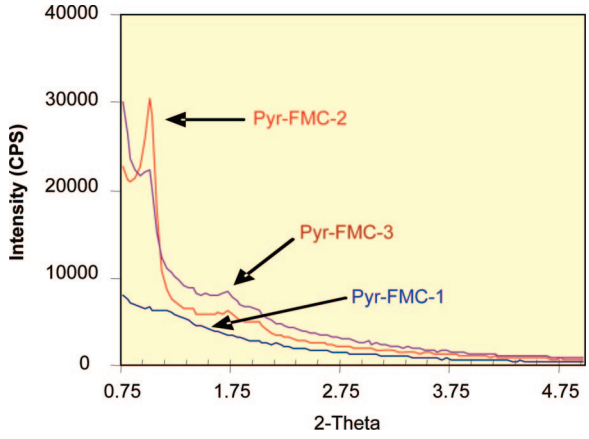

Figure 4. Low angle XRD of the pyridine functional mesoporous carbons (Pyr-FMC) made from the diethynylpyridines (Pyr-FMC-1 was made from 2,6-diethynylpyridine; Pyr-FMC-2 was made from 3,5-diethynylpyridine; and Pyr-FMC-3 was made from 2,5-diethynylpyridine).

pore size distribution is the result of two different templating mechanisms. The smaller pore size correlates with the wall thickness of SBA-15 materials (reported as 3.8 nm[35] and measured in this study at 2.7 nm) and is felt to be due to the pore structure exposed when the silica substrate is dissolved out from the carbonized intermediate. The larger pore size correlates nicely with the predicted pore diameter one would obtain by coating a 93 Å pore with a monolayer of diethynylpyridine molecules and polymerizing them. Thus, these pore size distribution data suggest that the Pyr-FMC-2 and Pyr-FMC-3 more faithfully preserve the structural features of the starting SBA-15 template than does the Pyr-FMC-1.

It seems reasonable to postulate that the diethynylpyridine precursors spontaneously self-assemble on the silica surface with the basic nitrogen atoms hydrogen bound to the surface silanols. The orientation of the acetylene substituents would then subsequently be dictated by their distribution on the pyridine ring. The orientation of the acetylenes is expected to have an impact on how cleanly the cyclotrimerization reaction takes place and therefore on the structure of the resultant mesoporous carbon and its defect density. Each system will be discussed in turn.

2,6-Diethynylpyridine. When this reaction sequence was carried out using 2,6-diethynylpyridine, a product (Pyr-FMC-1) was obtained that was disordered and had the lowest surface area and lowest pore volume of any of the three diethynylpridine-derived products (in fact, the pore volume was lower than that of the SBA-15 template). The low angle XRD spectrum of Pyr-FMC-1 is shown in Figure 4. In this precursor, both of the acetylenes are immediately adjacent to the pyridine N atom and therefore may hinder the ability of the molecule to hydrogen bond with the surface silanols (see Figure 5).

To probe the impact that 2,6-disubstitution has on the ability of the pyridine nucleus to hydrogen bond with a surface silanol, a series of control experiments was undertaken. First, the IR spectrum of the bare SBA-15 was obtained to establish the frequency of the surface silanol OH stretching bands. The isolated silanol OH stretching band was observed at 3748 cm^{-1}, and the onset of absorbance for the aggregated OH stretching band was observed at 3062 cm^{-1}. Next, the surface was saturated with pyridine, and the IR spectrum was obtained to determine the magnitude of the frequency shift of the OH stretching bands due to the hydrogen bond formed between the surface silanols and the unhindered pyridine nucleus. The isolated silanol stretching band shifted to lower frequency by 7 cm^{-1} (to 3741 cm^{-1}), and the onset of absorbance for the aggregated OH stretching band shifted to lower frequency by over 500 cm^{-1} (to 2533 cm^{-1}). Both of these observations are consistent with the pyridine molecules forming hydrogen bonds with the surface silanols, thereby weakening the O-H bonds. A third spectrum was then obtained by saturating the SBA-15 surface with 2,6-lutidine (2,6-dimethylpyridine, chosen as a model system for the diethynyl analogue to avoid any interference from the acetylenic groups), and the frequency shift of the OH stretching band was similarly determined. The isolated silanol stretching band in the 2,6-lutidine sample shifted to lower frequency by 13 cm^{-1} (to 3735 cm^{-1}), and the onset of absorbance for the aggregated OH stretching band shifted to lower frequency by several hundred cm^{-1} (it was not possible to precisely determine the exact position of this onset because of the broadness of the peak, but it was approximately 2500 cm^{-1}). It is clear from these spectroscopic results that both pyridine and 2,6-lutidine hydrogen bond to the surface silanols on SBA-15, and it does not appear that 2,6-disubstitution on the pyridine nucleus significantly hinders this hydrogen bonding ability. On the basis of these spectroscopic results, we postulate that the 2,6-diethynylpyridine still self-assembles on the silica surface, driven by the formation of hydrogen bonds between the pyridine N atom and the surface silanol.

Given that 2,6-diethynylpyridine is able to hydrogen bond with the surface silanols of SBA-15, it seems reasonable to postulate that the steric congestion induced by forcing the acetylenic groups into the silica surface would then lead to a somewhat more disordered arrangement of molecules on the surface. This disordered array may have an impact on the polymerization process and lead to more structural defects in the final product. This product (Pyr-FMC-1) was found by XPS analysis to contain 4.7% N, indicating that some degree of denitrogenation was taking place, most likely by some kind of ring fusion chemistry during carbonization. Similar denitrogenation chemistry has been reported in the production of carbon fibers from poly(acrylonitrile).[36] The relatively low surface area and low pore volume seem to indicate a relatively thick-walled structure. This would be consistent with either partial mesoporous collapse or a multiwalled structure. Either of these possibilities is consistent with the higher defect density predicted by this model, leading to a less rigid polymer intermediate going into the carbonization process.

3,5-Diethynylpyridine. When this process was carried out using 3,5-diethynylpyridine as the precursor, a cleanly ordered product (Pyr-FMC-2) was obtained that had mod-

(36) Bahl, O. P.; Shen, Z.; Lavin, J. G.; Ross, R. A. Manufacture of Carbon Fibers. In *Carbon Fibers*, 3rd ed.; Donnet, J. B., Wang, T. K., Rebouillat, S., Peng, J. C. M., Eds.; Marcel-Dekker: New York, 1998; pp 1–83.

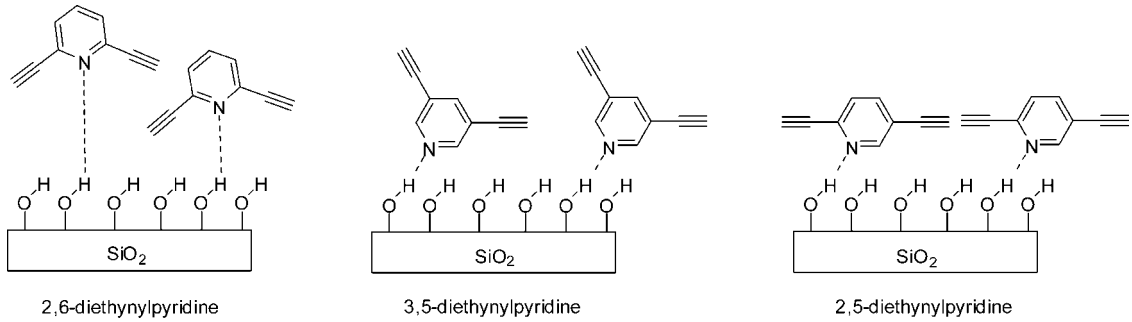

Figure 5. Depiction of the preassembly complexes formed between the various diethynylpyridines and a silica surface.

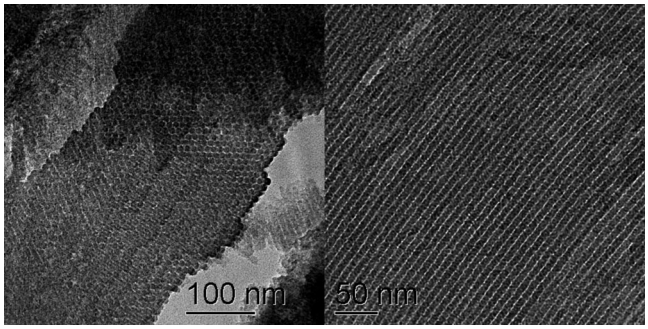

Figure 6. TEM images of Pyr-FMC-2, derived from the 3,5-diethynylpyridine precursor (left, hexagonal pore symmetry; right, cross section showing the ordered channel structure).

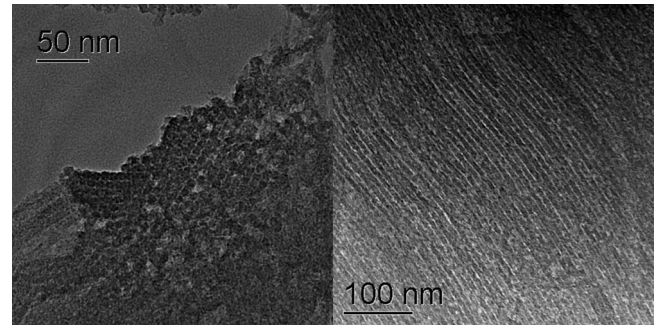

Figure 7. TEM showing the partially ordered structure of Pyr-FMC-3, derived from the 2,5-diethynylpyridine precursor (left, the partially ordered hexagonal symmetry; right, cross-section showing the ordered channel structure).

erately high surface area and pore volume (in this case, the pore volume was slightly higher than that of the SBA-15 template). The low angle XRD of Pyr-FMC-2 is shown in Figure 4. The strong, sharply defined peak at a 2θ of about 1.1°, along with the weaker features seen between about 1.5° and 2.0°, are consistent with an ordered hexagonal pore structure. This hexagonal pore structure is confirmed in the TEM micrographs shown in Figure 6. Note also the well-ordered channel structure shown in cross-section in Figure 6. Clearly, 3,5-diethynylpyridine is able to self-assemble in a way that is much better able to preserve the original SBA-15 structure than is the previously discussed 2,6 isomer. A linear hydrogen bond between the surface silanol and the pyridine N atom would result in the conformation shown in Figure 5. Note that this conformation places the two acetylene groups in different planes, opening the possibility that the "upper" acetylene might be available for multilayer formation arising from any "bulk" diethynylpyridine physisorbed on top of the hydrogen bound monolayer. XPS analysis of the product (Pyr-FMC-2) revealed that it contained approximately 3.5% N, indicating that some of the N functionality was lost, as in the previous example. The intermediate surface area and pore volume suggest that Pyr-FMC-2 may be a thick-walled (or multiwalled) structure. The observed loss of N functionality is consistent with this and suggests the possibility of this thick-walled structure being obtained via some sort of ring fusion chemistry.[36] In any event, the original ordered structure of the SBA-15 template is preserved in the Pyr-FMC-2 product.

2,5-Diethynylpyridine. When this process was carried out using 2,5-diethynylpyridine, a product (Pyr-FMC-3) was obtained with extremely high surface area and pore volume. In this case the pore volume was substantially higher than the original SBA-15 template. The XRD spectrum still shows the features consistent with hexagonal ordering (see Figure 4). While the TEM shows this hexagonal ordering, it does not show it as clearly as it did for the Pyr-FMC-2 (see Figure 7). However, TEM does show a clearly ordered channel structure in the cross section. On the basis of the extremely high surface area and pore volume, this self-assembly posture seems to be well-suited to the creation of what appear to be single-walled structures. These results can be rationalized in terms of the precursor posture on the silica surface (see Figure 5). With a linear hydrogen bond formed between the surface silanol and the pyridine nitrogen atom, the 2,5-diethynylpyridine molecule is allowed to adopt a "reclining" posture in which both of the acetylene groups are more or less parallel with the silica surface, making them ideally oriented for the cyclotrimerization reaction and less accessible for multilayer formation. This conformation appears to be very well-suited to this sort of pre-organized polymerization reaction. The Pyr-FMC-3 product was found by XPS analysis to contain 4.0% N, so once again, a significant portion of the N functionality was lost in the carbonization step, suggesting some degree of ring fusion is taking place at 800 °C. In any event, the 2,5-disubstitution pattern on the starting pyridine precursor clearly provides the greatest advantage in terms of surface area and pore volume of the final product, although interestingly enough, it does so with somewhat lesser preservation of pore symmetry.

It was hoped that by linking the pyridine units together through benzene linkers, it might be possible to inhibit the loss of N functionality by preventing the depolymerization process. The starting materials contain 11% N, and the products were found to contain between 3.5% N and 4.7%

N, indicating that a little over half of the N functionality was lost in the synthesis. While depolymerization appears to be unlikely in the initially formed materials, it appears that ring−ring condensation is still taking place at elevated temperatures of carbonization, leading to a loss of some of the N functionality. It was pointed out by a reviewer that it might also be possible that some of the N might have been lost during the HF wash. However, because the N functionality is in the form of pyridine ring systems, which are stable toward HF, we believe this route to be of little importance in this instance (for other more labile forms of N functionality, for example, benzylic amines, this mechanism of N loss would clearly need to be considered). We are currently exploring the possibilities of using lower reaction temperatures and transition metal catalysts in an effort to perform this chemistry with greater retention of functionality.

Conclusions

The thermal polymerization of arylacetylenes offers a simple and convenient method for making functional mesoporous carbons containing specific heteroaromatic functionality. The regiochemistry of the diethynylpyridine monomer and the stereochemistry of the self-assembled monolayer formed by these monomers hydrogen bonding to the surface of the silica template play an important role in dictating the structure and properties of FMCs obtained by this chemistry.

There are two competing mechansims at play in this chemistry, that of maintaining template structure (pore symmetry) and that responsible for creating a high surface area FMC. These two mechanisms appear to operate independently of one another. Maintaining the template structure is a reflection of how well the precursor can self-assemble into an ordered monolayer on the template interface. The creation of a high surface area FMC is dependent on monolayer versus multilayer polymerization and whether or not the product is a single-walled FMC or a thick-walled FMC. The orientation of the ethynyl moieties in the self-assembled precursor complex plays a role in both of these processes.

Acknowledgment. Parts of this work were performed at Pacific Northwest National Laboratories, which is operated for the US-DOE by Battelle Memorial Institute under contract DE AC06-76RLO 1830. This research was supported at PNNL by the Laboratory Directed Research and Development Program and the Office of Basic Energy Sciences, Division of Materials and Engineering, U.S. Department of Energy, and at the University of Oregon by the National Science Foundation (CHE-0414175 and -0718242). CAJ acknowledges the University of Oregon for a Doctoral Research Fellowship.

Supporting Information Available: Low angle XRD spectrum, absorption isotherm data for the surface area analysis, and pore size distribution of the SBA-15 template (PDF). This material is available free of charge via the Internet at http://pubs.acs.org.

CM070979O